A Statin-Loaded Reconstituted High-Density Lipoprotein Nanoparticle Inhibits Atherosclerotic Plaque Inflammation

Published in final edited form as:
Nat Commun. 2014 ; 5: 3065. doi:10.1038/ncomms4065.

A Statin-Loaded Reconstituted High-Density Lipoprotein Nanoparticle Inhibits Atherosclerotic Plaque Inflammation

Raphaël Duivenvoorden[1,2,12], **Jun Tang**[1,3,12], **David P. Cormode**[1,4], **Aneta J. Mieszawska**[1], **David Izquierdo-Garcia**[1], **Canturk Ozcan**[1], **Maarten J. Otten**[1], **Neeha Zaidi**[1], **Mark E. Lobatto**[1,2], **Sarian M. van Rijs**[1], **Bram Priem**[1], **Emma L. Kuan**[5], **Catherine Martel**[6], **Bernd Hewing**[7,8], **Hendrik Sager**[9], **Matthias Nahrendorf**[9], **Gwendalyn J. Randolph**[6], **Erik S.G. Stroes**[2], **Valentin Fuster**[10,11], **Edward A. Fisher**[7], **Zahi A. Fayad**[1], and **Willem J.M. Mulder**[1,2]

[1]Translational and Molecular Imaging Institute, Icahn School of Medicine at Mount Sinai, New York, NY, USA [2]Department of Vascular Medicine, Academic Medical Center, Amsterdam, The Netherlands [3]Graduate School of Biomedical Sciences, Icahn School of Medicine at Mount Sinai, New York, NY, USA [5]Department of Gene and Cell Medicine and Institute for Immunology, Icahn School of Medicine at Mount Sinai, New York, NY, USA [6]Department of Pathology & Immunology, Washington University in St. Louis, St. Louis, Missouri, USA [7]Department of Medicine (Cardiology) and Cell Biology, Marc and Ruti Bell Program in Vascular Biology, NYU School of Medicine, New York, USA [8]Medizinische Klinik für Kardiologie und Angiologie, Campus Mitte, Charité – Universitaetsmedizin Berlin, Berlin, Germany [9]Center for Systems Biology, Massachusetts General Hospital, and Division of Cardiovascular Medicine, Brigham and Women's Hospital, Harvard Medical School, Boston, MA [10]Department of Cardiology, Zena and Michael A. Weiner Cardiovascular Institute and Marie-Josée and Henry R. Kravis Cardiovascular Health Center, Icahn School of Medicine at Mount Sinai, New York, USA [11]Centro Nacional de Investigaciones Cardiovasculares (CNIC), Madrid, Spain

Abstract

Inflammation is a key feature of atherosclerosis and a target for therapy. Statins have potent anti-inflammatory properties but these cannot be fully exploited with oral statin therapy due to low systemic bioavailability. Here we present an injectable reconstituted high-density lipoprotein

Corresponding Author: Willem Mulder, PhD, Translational and Molecular Imaging Institute, Icahn School of Medicine at Mount Sinai, One Gustave L. Levy Place, P. O. Box 1234, New York, NY 10029; USA, willem.mulder@mssm.edu.
[4]Current Address: Department of Radiology, University of Pennsylvania Perelman School of Medicine, Philadelphia, PA 19104, USA
[12]These authors contributed equally to this work.

Author Contributions. R.D., J.T. and W.J.M.M. designed the experiments with help from Z.A.F., E.F., V.F., G.J.R. and E.S.G.. W.J.M.M., D.P.C., N.Z. and J.T. developed the rHDL nanoparticles. J.T. synthesized the nanoparticles and performed the TEM, dynamic light scattering, and *in vitro* experiments with help from D.P.C.. Flow cytometry was performed and analysed by J.T., C.M. and E.L.K, supervised by G.J.R.. R.D. and J.T. performed the MRI, NIRF, bright field and fluorescent microscopy with help of M.L., M.J.O. and S.M.v.R.. R.D. and J.T. performed the serum lipid and FPLC measurements, supervised by E.F.. D.I.G. wrote the analysis software for the microscopy image analysis. R.D. processed the MRI and histology data. J.T., B.H. and B.P. performed the laser capture microdissection analysis experiments. J.T., A.J.M. and C.O. performed the HPLC studies. FMT-CT experiments were performed by J.T. and H.S., and supervised by M.N.. R.D., J.T. and W.J.M.M. wrote the manuscript. All authors discussed the results and commented on the manuscript. W.J.M.M. and Z.A.F. were responsible for the overall supervision of the study.

Conflict of interest. There is disclosure for conflict of interest

(rHDL) nanoparticle carrier vehicle that delivers statins to atherosclerotic plaques. We demonstrate the anti-inflammatory effect of statin-rHDL *in vitro* and show this effect is mediated through inhibition of the mevalonate pathway. We also apply statin-rHDL nanoparticles *in vivo* in an apolipoprotein E-knockout mouse model of atherosclerosis and show they accumulate in atherosclerotic lesions where they directly affect plaque macrophages. Finally we demonstrate that a three-month low-dose statin-rHDL treatment regimen inhibits plaque inflammation progression, while a one-week high-dose regimen markedly decreases inflammation in advanced atherosclerotic plaques. Statin-rHDL represents a novel potent atherosclerosis nanotherapy that directly affects plaque inflammation.

Introduction

Atherosclerotic diseases, such as acute myocardial infarction, are a major cause of death and disability worldwide [http://www.who.int/cardiovascular_diseases/en/]. Preventive strategies currently focus on controlling risk factors, such as smoking, blood pressure, serum glucose and lipid levels[1]. Despite the success of these preventive measures, substantial residual risk remains even when treatment goals are fully met[2]. In patients that suffered a myocardial infarction the recurrence risk of an acute coronary syndrome is high, particularly within the first year when recurrence rates are up to 17.4%[3]. A recent study explained this phenomenon by showing that a systemic response to ischemic injury aggravates inflammation in atherosclerotic plaques at a distance, due to increased monocyte recruitment[4]. Monocytes that infiltrate the plaque differentiate into macrophages, which produce proteolytic enzymes that digest extracellular matrix causing plaque rupture[5]. The immediate site of plaque rupture contains a high concentration of inflammatory cells[6]. Plaque inflammation is therefore pursued as a therapeutic target to prevent atherothrombotic events[7].

In the current study we developed a nanomedicine-based delivery strategy based on reconstituted high density lipoprotein (rHDL) nanoparticles that allow for drug delivery to atherosclerotic plaques. As a cargo for our rHDL nanoparticles we selected a 3-hydroxy-3-methylglutaryl coenzyme A reductase (HMGR) inhibitor, or statin. Statins are widely orally prescribed serum low density-lipoprotein (LDL) cholesterol-lowering drugs that upregulate LDL receptor expression in hepatocytes[8]. In addition to its effect on hepatocytes, various studies have established the potent immunomodulating effects of HMGR inhibition in inflammatory cells[9–11]. In an atherosclerotic mouse model in which statins did not affect lipid levels, reduced plaque formation was shown with extremely high doses of oral statin therapy[12]. However, in humans increasing the oral statin dose to attain higher plasma concentrations is not feasible due to the dose-dependent onset of adverse effects such as hepatoxicity and myopathy[13]. Normal doses of orally ingested statins hardly enter the systemic circulation as biotransformation occurs in the liver[14].

We addressed this issue by developing a statin-loaded rHDL nanoparticle ([S]-rHDL) that can be administered intravenously, augments bioavailability, and facilitates the delivery of statins to atherosclerotic plaque. We show, in an apolipoprotein E-knockout (apoE-KO) mouse model of atherosclerosis, that a three-month low dose- as well as a one-week high dose [S]-rHDL treatment regimen markedly reduces plaque macrophage content.

Results

Study summary

A schematic overview of the study design is shown in Fig 1. First, we studied [S]-rHDL's characteristics and its efficacy in different cell lines *in vitro*. Subsequently, biodistribution and toxicity, as well as uptake by atherosclerotic plaque macrophages were investigated in mouse models *in vivo*. Next, we investigated the in vivo efficacy of a low dose long-term [S]-rHDL infusion regimen on plaque development and a short-term high dose infusion regimen on plaque regression in apoE-KO mice.

[S]-rHDL characteristics

We constructed [S]-rHDL from recombinant human apolipoprotein A-1 (ApoA-1), the phospholipids 1-myristoyl-2-hydroxy-sn-glycero-phosphocholine (MHPC) and 1,2-dimyristoyl-sn-glycero-3-phosphatidylcholine (DMPC), in which lipophilic simvastatin was encapsulated. This resulted in discoid-shaped nanoparticles of 25 to 30 nm in diameter as determined by dynamic light scattering and transmission electron microscopy (Fig. 2a, Supplementary Fig. S1, and Supplementary Table S1). Its exact composition was established by phosphate determinations and simvastatin measurements by high-performance liquid chromatography (Supplementary Table S1). Stability experiments with the free drug and the [S]-rHDL nanoparticle formulation in mouse serum demonstrated the protective function of the rHDL nanoparticle towards statin degradation (Supplementary Fig. S2). To allow its visualization in cells and tissue via imaging techniques we also synthesized a variant where an amphiphilic MRI contrast agent, gadolinium - diethylene triamine pentaacetic acid-distearyl amide (Gd-DTPA-DSA) and/or fluorescent dyes (Cy5.5, DiO or DiR) were incorporated (Fig. 2a).

In vitro efficacy of [S]-rHDL

To assess [S]-rHDL's therapeutic potential and function we investigated its anti-inflammatory effect *in vitro*. First, we investigated the effect of [S]-rHDL on viability of murine macrophages (J774A.1) as well as on hepatocytes, endothelial cells and smooth muscle cells as function of incubation concentration and time. Cells were incubated with rHDL or [S]-rHDL, with statin doses of 1 μM, 10 μM and 100 μM (Supplementary Fig. S3). Macrophage survival was comparable in the rHDL and [S]-rHDL incubated cells at 6 and 12 hour time points, while macrophage survival decreased in the [S]-rHDL incubated cells at 24 and 48 hours. A similar response was observed in cultured endothelial cells. Significantly less loss in cell viability was observed for the smooth muscle cells and hepatocytes (Supplementary Fig. S3). Subsequently, we investigated if the effect of [S]-rHDL on macrophage cell viability was mediated through the mevalonate pathway. In macrophages incubated with [S]-rHDL or free statin (10 μM), we observed a nearly complete loss of cell viability at 48 hours incubation time, while this did not occur in cells incubated with rHDL. This effect was abolished when mevalonate was added to [S]-rHDL or free statin (Fig. 2b). Next, we evaluated [S]-rHDL's effect on the expression of inflammatory cytokines (Fig. 2c). We first stimulated the macrophages with LPS and IFN-γ for 16 hours. Cell viability at these conditions was not markedly affected. We then treated the cells with different treatments for 24 hours in serum-free condition, and assessed expression of the anti-

inflammatory markers monocyte chemotactic protein-1 (MCP-1) and tumor necrosis factor-α (TNF-α). We observed a decrease in expression of MCP-1 and TNF-α in macrophages treated with [S]-rHDL or free statins. The expression of MCP-1 and TNF-α was restored by the addition of mevalonate in macrophages treated with [S]-rHDL and free statins (Fig. 2c). Cell viability of macrophages treated with [S]-rHDL was similar to control cells (Supplementary Fig. S4). These data show that [S]-rHDL reduces cell viability and the production of inflammatory cytokines by inhibiting the mevalonate pathway. Subsequently, we investigated the mechanism by which [S]-rHDL decreases macrophage cell viability. We observed that [S]-rHDL decreased macrophage proliferation. We also observed that [S]-rHDL causes non-apoptotic macrophage cell death (Supplementary Fig. S4).

In vivo biodistribution and toxicity studies

To investigate [S]-rHDL's biodistribution we designed an [S]-rHDL nanoparticle that carried 2 labels, namely Cy5.5 conjugated to a phospholipid and the hydrophobic dye DiO or DiR. Cy5.5-phospholipids incorporated in the corona, while the hydrophobic dyes DiO / DiR were incorporated in the simvastatin-loaded core of [S]-rHDL (Fig. 2a). Lipoproteins, including HDL, are dynamic systems that are known to exchange lipid components[15–17]. Therefore, we hypothesized that the hydrophobic DiO / DiR core label would display a different kinetic behaviour from the amphiphilic phospholipid-Cy5.5 corona label. To investigate this, we injected apoE-KO mice (N=21) with the dual-labelled [S]-rHDL, sacrificed at different time points (N=3 per time point), and collected the blood, hearts, aortas, spleens, livers and kidneys. The blood was separated into three fractions, i.e. plasma, mononuclear cells (MNC) and red blood cells (RBC). We observed that the majority of the Cy5.5 labelled phospholipids remained in the plasma fraction of the blood, while a small fraction was transferred to the RBC (Fig. 3a and b). The core label DiO was detectable in the serum fraction only and displayed longer circulation kinetics. Further analysis of blood by flow cytometry revealed the small fraction of DiO associated with MNC to be most abundantly present in pro-inflammatory Gr-1^{hi} monocytes (Fig. 3c, Supplementary Fig. S5).

Near infrared fluorescence (NIRF) imaging and fluorescence microscopy of the spleen, liver and kidneys revealed the highest DiR presence in liver tissue (Supplementary Fig. S6). Nanoparticles were found in heart, aorta, liver, spleen, and kidney tissue, but not in muscle tissue (Supplementary Fig. S6). A combination of restricted nanoparticle accessibility from the muscle microvasculature to muscle tissue and the absence of SR-B1, ABCA-1 or ABCG-1 expression may explain why our nanoparticle were not found associated with myocytes. In the spleen, DiR signal co-localized with CD68-stained monocytes/macrophages (Supplementary Fig. S7). Flow cytometry analysis of spleen cells revealed that macrophages and Ly-6c^{hi} (Gr-1^{hi}) monocytes took up [DiO-S]-rHDL most efficiently, while neutrophils and Ly-6c^{lo} (Gr-1^{hi}) moncoytes took up markedly less nanoparticles. [S]-rHDL did not exert toxic effects on liver, kidney or myocytes when it was administered to mice at a high dose (60 mg/kg simvastatin, 40 mg/kg ApoA-1, 4 intravenous infusion / week) for a week (Supplementary Fig. S8).

Accumulation and uptake in atherosclerotic plaques

To assess whether our nanoparticles accumulated in atherosclerotic lesions and was taken up by plaque macrophages, we conducted two experiments. In the first experiment, apoE-KO mice on a high cholesterol diet for 28 weeks, were infused with gadolinium and statin containing rHDL ([Gd-S]-rHDL, N=3), or placebo (N=3). *In vivo* MRI experiments performed with a 9.4 Tesla scanner revealed signal enhancement in the vessel wall on T1-weighted images 24 hours after infusion of [Gd-S]-rHDL, indicating pronounced accumulation of our nanoparticle in the vessel wall (Fig. 2d).

In the second experiment dual-labelled [S]-rHDL, with Cy5.5-phospholipids in the corona and DiO / DiR in the core, were injected in apoE-KO mice. 24 hours post-injection, the mice were sacrificed and the hearts and aortas were excised. The distribution of DiR labelled [S]-rHDL in intact aortas was investigated by NIRF imaging and revealed its accumulation in regions rich in plaques (Fig. 3e). The targeting kinetics of DiO (the core label) and Cy5.5-phospholipid label displayed a pattern similar to the blood kinetics (Fig. 3f), namely that the Cy5.5-labelled phospholipids appeared in the plaque until 4 hours post injection after which their presence declined. In contrast, the DiO core label was retained in the plaque up to at least 24 hours. Furthermore, fluorescence microscopy of plaques revealed co-localization of DiO-labelled [S]-rHDL with macrophages in the aortic root (Fig. 3g). Flow cytometry of cells from atherosclerotic plaques showed that the fluorescence intensity of the core label DiO was 5–6 fold stronger in macrophages (MΦ) than in freshly recruited monocytes (Mo) (Fig. 3h, Supplementary Fig. S5).

In vivo efficacy of low dose [S]-rHDL infusions

To investigate the effect of [S]-rHDL on plaque inflammation we used apoE-KO mice (N=74) that were on a high cholesterol diet for 14 weeks in order to develop atherosclerosis. Statins are known not to affect blood cholesterol levels of apoE-KO mice, because they lack the major ligand for the LDL receptor, namely apoE[18,19], and also metabolize statins very fast in their livers[20], making this a suitable model to solely investigate the anti-inflammatory effects of HMGR inhibition. To limit a dominant therapeutic effect of rHDL itself, we used a low ApoA-1 dose. While the mice remained on the high cholesterol diet, they received bi-weekly infusions of [S]-rHDL (15 mg/kg statin, 10 mg/kg ApoA1, N=16), placebo (saline infusion, N=15), orally dosed statin (15 mg/kg statin daily, N=15) or bi-weekly infusion of bare rHDL nanoparticles (10 mg/kg ApoA1, N=15) for 12 consecutive weeks. We also included a group of mice that were sacrificed when the other groups started their treatment, which we refer to as the baseline group (N=12). As plaque formation in apoE-KO mice occurs more rapidly in the aortic root than in the abdominal aorta we were able to study the effects of [S]-rHDL in both early and established atherosclerotic lesions. In the aortic root plaque formation is reproducible, consistent and homogenous, and covers a length of less than 0.5 mm, which enables us to apply quantitative histology analyses. We evaluated 42 cross-sections of the aortic sinus area per mouse. This resulted in the analysis of 3108 cross-sections in total. Cross-sections were stained for connective tissue with hematoxylin phloxine saffron (HPS) or immunostained with CD68 antibodies to visualize macrophages. We developed a quantitative and digitized method with in-house developed software (Matlab) for the analysis of the histology images, to quantify total plaque area (macrophages

plus connective tissue) and macrophage rich area (Supplementary Fig. S9). In contrast to the development of atherosclerosis in the aortic root, plaque formation in the abdominal aorta is heterogeneous and covers a length of 2 cm, which excludes histological analysis for an accurate assessment. Instead we performed longitudinal *in vivo* 9.4 T MRI in a subset of mice (N=40, 7–9 per group, Supplementary Fig. S10). Examples of histological sections of the abdominal aorta are displayed in Supplementary Fig. S11.

Our *in vivo* MRI data showed that compared to the [S]-rHDL-treated group, vessel wall thickness was 16% higher in the placebo group (Mann-Whitney U test p=0.01), 12% higher in the oral statin group (Mann-Whitney U test p=0.004), and 16% higher in the rHDL group (Mann-Whitney U test p=0.005, Fig. 4a, b) at the end of the study.

Subsequently, all mice (N=74) were sacrificed and atherosclerotic burden was quantified by means of histology of the aortic sinus. Total plaque area in the [S]-rHDL group was significantly decreased by 34% compared to the baseline group (Mann-Whitney U test p<0.001), by 37% compared to placebo (Mann-Whitney U test p=0.002), and by 28% compared to rHDL (Mann-Whitney U test p=0.006, Fig. 4c). The [S]-rHDL group showed a trend towards a decrease of 17% compared to the oral statin group (Mann-Whitney U test p=0.06, Fig. 4c). Plaque macrophage content was markedly decreased in the [S]-rHDL group by 56% compared to the baseline group (Mann-Whitney U test p<0.001), by 57% compared to placebo (Mann-Whitney U test p=0.001), by 37% compared to oral statin (Mann-Whitney U test p=0.003), and by 40% compared to rHDL (Mann-Whitney U test p=0.03, Fig. 4d). In Fig. 4e typical and representative histological sections of the different groups are shown.

We also quantified the cholesterol content of the thoracic aortas of all mice (N=74), by digesting the excised aortas followed by chemical quantification of the cholesterol content. In line with expectation, we did not observe any differences in aorta cholesterol content across all groups (Supplementary Fig. S12).

Serum triglyceride and total cholesterol levels did not differ significantly across all groups, although total cholesterol had the tendency to be higher in the placebo and rHDL groups (Supplementary Fig. S13). Total cholesterol levels were equal in the oral statin and [S]-rHDL groups, however, fast-performance liquid chromatography showed that the oral statin group had a more favorable lipid profile than the [S]-rHDL group, with 31% lower VLDL, 16% lower LDL and 37% higher HDL cholesterol (Supplementary Fig. S14). The decrease in plaque macrophage area by [S]-rHDL remained significant compared to placebo (Multiple linear regression analysis p=0.002), oral statin (Multiple linear regression analysis p=0.01), and rHDL (Multiple linear regression analysis p=0.02) after statistical adjustment for serum total cholesterol levels.

In vivo efficacy of high dose [S]-rHDL infusions

To assess the effect of short term high dose [S]-rHDL therapy on plaque inflammation, apoE-KO mice that had developed advanced atherosclerotic lesions after 27 weeks of the high cholesterol diet, were administered high dose [S]-rHDL (60 mg/kg statin, 40 mg/kg ApoA1, N=7), placebo (saline infusion, N=15), high dose rHDL (40 mg/kg ApoA1, N=8),

or low dose [S]-rHDL (15 mg/kg statin, 10 mg/kg ApoA1, N=10). All mice (N=40) received four infusions of their assigned therapy within a single week. Histological assessment of the aortic sinus area was performed as described before (Supplementary Fig. S9), and a total of 1680 cross sections were analyzed. Histology showed a trend towards a decrease of 31% in total plaque area in the high dose [S]-rHDL-group compared to placebo (Mann-Whitney U test p=0.053), and was decreased by 34% compared to high dose rHDL (Mann-Whitney U test p=0.005), and by 36% compared to the low dose [S]-rHDL-group (Mann-Whitney U test p=0.006, Fig. 5a). The decrease in total plaque area primarily accounted for the decreased macrophage positive areas in the high dose [S]-rHDL-group. It was decreased by 84% when compared to placebo (Mann-Whitney U test p<0.001), by 79% compared to high dose rHDL (Mann-Whitney U test p=0.001), and 77% compared to low dose [S]-rHDL (Mann-Whitney U test p=0.002, Fig. 5b). In Fig. 5c typical and representative histological sections of the different groups are shown. Serum triglyceride and total cholesterol levels were equal across all groups (Supplementary Fig. S15). The difference in plaque macrophage content between the [S]-rHDL group and placebo (Multiple linear regression analysis p<0.001), oral statin (Multiple linear regression analysis p<0.001), and rHDL (Multiple linear regression analysis p=0.004) remained significant after statistical adjustment for serum total cholesterol levels.

In a subsequent study, also in apoE-KO mice (N=36) with advanced atherosclerosis, we determined the mRNA expression levels of genes related to inflammation in plaque macrophages by means of laser capture microdissection (LCM). We compared mice treated with high dose [S]-rHDL, to mice treated with oral statin therapy, and placebo (Fig. 5d, Supplementary Fig. S16). We observed that in the high dose [S]-rHDL group, mRNA expression levels of monocyte recruitment genes (MCP-1, CCL-3, ICAM-1, VCAM-1, CCL-15, CXCL-12), as well as those of pro-inflammatory genes (TNF-α, IL-1β, IL-1α, SPP-1), were markedly decreased as compared to the oral statin and placebo groups (Fig. 5d). The anti-inflammatory mannose receptor (MR) mRNA level was increased in the high dose [S]-rHDL group as compared to placebo, but was similar to the oral simvastatin group (Fig. 5d).

Finally, to corroborate these findings we performed *in vivo* fluorescence molecular tomography with computed tomography (FMT-CT) imaging to visualize and measure the protease activity in the aortic roots of another 11 apoE-KO mice. We revealed that the inflammatory protease activity was markedly reduced in apoE-KO mice treated with [S]-rHDL as compared to placebo (Fig. 5e). Together these data demonstrate the potent local anti-inflammatory effect of [S]-rHDL in atherosclerotic plaques.

Discussion

In the current study we described the development of a statin-rHDL nanoparticle as a therapy for reducing atherosclerotic plaque inflammation. The key findings of our study are that this compound (1) suppresses the inflammatory response of macrophages which is mediated through the inhibition of intracellular mevalonate pathway, (2) accumulates in atherosclerotic plaque where it is taken up by macrophages, (3) markedly reduces plaque

macrophage content and inflammation following both prolonged low dose therapy as well as short-term high dose therapy, and (4) does not exhibit myo- or hepatotoxic effects.

The platform on which we based our nanoparticle is rHDL. Traditionally, HDL is considered to remove excess cholesterol from peripheral tissues and transport it to the liver for fecal excretion, a process referred to as the "reverse cholesterol transport"[21,22]. For this reason previous studies have investigated rHDL as a therapeutic agent. Shah *et al*. showed that in apoE-KO mice, 18 infusions of 40 mg/kg ApoA1 within 5 weeks had no effect on plaque size, but reduced plaque lipid content by 40%, and plaque macrophage content by 46%[23]. In another study, Shah *et al*. showed in apoE- KO mice that a single injection of 400 mg/kg ApoA1 reduced plaque lipid content by 40–50% and plaque macrophage content by 29–36%[24]. It is important to note that in the current study we did not aim at employing rHDL and ApoA1 as a therapeutic agent, apart from its ability to deliver statin to plaque tissue. Compared to the studies by Shah *et al*. we used lower ApoA1 doses, namely 24 infusions of 10mg/kg in the 3 months low dose study and 4 infusions of 40 mg/kg ApoA1 in the single week high dose study. In both our low- and high dose study plaque size was unchanged in the rHDL-group as compared to placebo, but plaque macrophage content tended to be lower in the rHDL-groups as compared to placebo. Despite this, we were able to show a marked reduction in plaque macrophage content by [S]-rHDL treatment compared to the rHDL-group. rHDL infusion has also been investigated in large randomized controlled trials in humans[25,26]. Although the therapeutic efficacy was disappointing, the ApoA1 doses of 40 mg/kg used in these studies were well tolerated. This shows that the ApoA1 doses of 10 mg/kg and 40 mg/kg that we used can safely be translated to future human studies.

In addition to HDL's ability to remove excess cholesterol from atherosclerotic plaques, native HDL also transports proteins involved in inflammation, coagulation, complement activation[27], and endogenous micro RNAs, and delivers them to recipient cells[28]. This indicates that native HDL is in fact a carrier vehicle involved in complex intercellular communication. In the current study we utilize this natural property of HDL to act as a delivery vehicle of statins to target macrophages in atherosclerotic lesions. We showed that rHDL protects the statin cargo from catabolism in the serum, increases statin's bioavailability, and delivers its cargo to plaques where it is taken up by plaque macrophages. Our data on pharmacokinetics demonstrate that in the circulation [S]-rHDL is predominantly located in the plasma, and a small sub-fraction in blood monocytes. Blood monocytes that took up [S]-rHDL in the circulation and subsequently infiltrated the plaque, could potentially account for some of the accumulation of [S]-rHDL in the plaque. However, direct infiltration from the plasma into the plaque most likely accounts for the majority of [S]-rHDL accumulation in plaques. The reason why, within the vasculature, [S]-rHDL preferentially accumulates at sites of atherosclerotic lesions is likely related to local endothelial permeability, which facilitates infiltration of the nanoparticle into the vascular tissue, after which it is retained due to ingestion by macrophages. We did not investigate the mechanism by which plaque macrophages take up [S]-rHDL. Native HDL is known to interact with macrophages through scavenger receptor B1, and adenosine triphosphate binding cassette transporter A1 and G1[21,22]. Possibly our nanoparticle has a similar interaction or is simply phagocytosed by macrophages.

The current study is the first to pursue local delivery of statins to plaque tissue to achieve local anti-inflammatory effects. The immunomodulating effects of statins have been established in previous studies, which showed that HMGR inhibition reduces the production of downstream isoprenoid intermediates (e.g. farnesyl pyrophosphate) in the intracellular cholesterol synthesis pathway, which decreases the isoprenylation of proteins[29,30]. This interferes with the attachment of proteins to the cell membrane, which affects proliferation and function of inflammatory cells, such as macrophages[9–11]. In the current study we confirm the anti-inflammatory effect of statins both *in vitro* and *in vivo. In vitro*, we show that the anti-inflammatory effect remains equally potent when statin is encapsulated in rHDL as compared to free statin. We also demonstrate that the anti-inflammatory effects of statins are mediated through the inhibition of the mevalonate pathway, which corroborates results from previous studies[9–11].

A previous study in an atherosclerotic mouse model investigated the effects of oral statin therapy on atherogenesis. Sparrow *et al*. treated apoE-KO mice daily with 100 mg/kg simvastatin for 6 weeks, and showed marked reduction in aortic plaque development despite the fact that statin therapy did not affect serum lipid levels[12]. They also showed effects of their high dose oral statin therapy on carrageenan-induced foot pad edema, a model of inflammation. They did not investigate the mechanism by which atherogenesis and inflammation was reduced, but it is conceivable that higher than normal serum levels of statins were achieved since their oral statin dose was extremely high. In humans it is not possible to administer such high oral doses due to adverse effects[13]. In the current study we used a lower oral statin dose than that used by Sparrow *et al*., namely 15 mg/kg in the 3 months low dose study. Plaque size and macrophage content tended to be lower in the oral statin group compared to placebo. Nonetheless, we showed a marked reduction in plaque inflammation with [S]-rHDL treatment, despite 3.5 times lower weekly doses of statin in [S]-rHDL-group (15 mg/kg simvastatin, 2 times / week) than that in oral statin-group (15 mg/kg simvastatin / day).

In addition to the decrease in plaque macrophage content following [S]-rHDL treatment, we were able to show that [S]-rHDL markedly affects plaque macrophage mRNA expression levels of genes related to inflammation. Furthermore, we observed that short-term high-dose [S]-rHDL treatment markedly decreased inflammatory protease activity in atherosclerotic plaques, which was measured *in vivo* with FMT-CT.

Of note, in the current study we focused on the anti-inflammatory effect of our nanoparticle, since statins do not affect serum lipid levels in this mouse model. However, we showed that in the mice nanoparticles were taken up in the liver. In humans [S]-rHDL will undoubtedly also be taken up by hepatocytes, where the delivered statin will up-regulate the LDL-receptor expression. Thus in humans, our nanoparticle may have two therapeutic effects, namely an anti-inflammatory effect on plaques as well as a cholesterol lowering effect due to its effect on hepatocytes.

The clinical implications of our findings pertain to the field of cardiovascular disease. With current standard of care therapy, recurrent angina before discharge occurs in up to 10% of patients following an acute coronary syndrome, and recurrent acute coronary syndrome

within the first year in 17.4% of patients[3]. Therefore novel therapeutic strategies like rHDL infusion are being developed, with the concept to initiate therapy directly after the acute event in an effort to rapidly decrease plaque vulnerability. Unfortunately, the efficacy of rHDL infusion alone so far has been disappointing[25,26]. Extrapolating from the evidence provided, we envision that [S]-rHDL nanotherapy can facilitate plaque retention of high quantities of statin following short-term intravenous administration in acute coronary syndrome patients, thereby modulating plaque inflammation[31]. This holds promise to suppress plaque inflammation during the vulnerable period following acute coronary syndrome, which can support standard-of-care therapy to prevent recurrent plaque rupture and atherothrombotic events. An advantage of nanotherapy we present is that the individual components are well tolerated by humans. Statins are prescribed routinely to millions of patients worldwide, whereas rHDL in lower concentrations has proven to be safe in large phase IIB trials[13,25,26]. In our study we did not observe myo- or hepatotoxicity of our nanoparticle. Therefore, [S]-rHDL represents a novel anti-atherosclerotic nanotherapy with a high potential for clinical translation.

In conclusion, [S]-rHDL nanotherapy locally treats atherosclerotic inflammation at the level of the vessel wall. The potency of the treatment allows for the inhibition of plaque inflammation using a long-term, low-dose treatment regimen, while a short-term, high-dose treatment regimen can be applied to rapidly deplete inflammation in advanced atherosclerotic plaques.

Methods

Synthesis of [S]-rHDL

The synthesis of [S]-rHDL was modified from a published method[32]. Briefly, simvastatin (AKscentific), 1-myristoyl-2-hydroxy-sn-glycero-phosphocholine (MHPC) and 1, 2-dimyristoyl-sn-glycero-3-phosphatidylcholine (DMPC) (both purchased from Avanti Polar Lipids) were dissolved in chloroform/methanol (4:1 by volume) solvent and dried to form thin film. Human apolipoprotein A1 proteins (ApoA-1) (CSL, Parkville, Australia) dissolved in PBS was added to the film and the solution was incubated in 37°C till the film was hydrated and a homogenous solution was formed. The solution was sonicated to form small [S]-rHDL nanoparticles. Aggregates were removed by centrifugation and filtration. Gadolinium-DTPA-DMPE (Avanti Polar Lipids), Cy5.5-DMPE (DMPE was conjugated with Cy5.5 NHS-ester purchased from GE healthcare), DiR or DiO (Invitrogen) were added when the nanoparticles were subsequently used for imaging purposes. Control rHDL nanoparticles without simvastatin were synthesized with the same procedures.

Characterization of [S]-rHDL

Nanoparticles were negatively stained with a method previously reported[33]. Images were acquired using a Hitachi H7650 system linked to a SIA (Scientific Instruments and Applications) digital camera controlled by Maxim CCD software. The mean size of the different formulations of nanoparticles was determined by dynamic light scattering (Brookhaven Instruments Corporation, Holtsville, NY) and by measuring the nanoparticles in transmission electron microscopy (TEM) images. The percentage of phospholipids in the

nanoparticles was determined by Rouser's method; the percentage of simvastatin by high performance liquid chromatography (HPLC) (Shimadzu HPLC instrument); the percentage of protein by a BCA protein concentration assay (Bio Rad); The longitudinal relaxivity (r1) of gadolinium loaded [S]-rHDL ([Gd-dye-S]-rHDL) were measured on a 60 MHz Bruker Minispec (Bruker Medical BmbH, Ettingen) operating at 40 °C. To determine the half-life of encapsulated simvastatin in [S]-rHDL, a concentration of 1000 μg/ml of simvastatin from [S]-rHDL or free simvastatin was achieved in mouse serum and the solution was kept at 37 °C. The concentration of intact simvastatin in the serum at different time points was measured with HPLC) (Shimadzu HPLC equipped with a column (Ascentis C18, 10 cm x 4.6 mm I.D., 3 μm particles (581321-U) Reversed phase), using a protocol adapted from the published one[34]. The mobile phase was 80% Acetonitrile and 20% H_2O and flow rate was 0.5 ml/min. The half-life of simvastatin in [S]-rHDL and free simvastatin was defined as the length of incubation time when the serum simvastatin concentration was 500 μg/ml.

In vitro cell assays

J774A.1 (murine macrophages), MS1 (murine endothelial cells), MOVAS (murine aortic smooth muscle cells) and Hepa-1c1c7 (murine liver cells) were cultured under ATCC-recommended conditions. [S]-rHDL nanoparticles were added to the cells to reach different concentrations of simvastatin in cell culture, whereas rHDL nanoparticles were added to reach the same ApoA-1 concentrations as [S]-rHDL in each condition, and mevalonate was added to reach 100 μM when needed. The cell viability was determined by measuring intracellular ATP concentration by following the manufacturer's instructions (Promega, CellTiter Glo). To measure MCP-1 and TNF-α production by J774A.1 cells, the cells were first challenged with LPS and IFN-γ for 16 hours, and subsequently switched to serum-free culture condition and treated with [S]-rHDL, free simvastatin, rHDL or nothing for another 24 hours at the concentration of 10 μM simvastatin or equal concentration of ApoA-1 from rHDL, in the presence or absence of 100 μM mevalonate. TNF-α and MCP-1 concentrations in the supernatants were measured with ELISA by following the manufacturer's instructions (Biolegend).

For apoptosis/necrosis assay, murine cells (J774A.1) were treated with 10 μM simvastatin equivalent [S]-rHDL for 24 hours, and then stained with either apoptosis specific dye (YO-PRO-1) or necrosis specific dye (Propidium iodide). Measurement was used following manufacture's instruction (life technologies, Cat# V13243). In brief, apoptotic cells are defined as YO-PRO-1 positive Propidium iodide positive on flow cytometry graph, while necrosis cells are YO-PRO-1 negative Propidium iodide positive. For cell proliferation, assay was done by following the manufacturer's instruction (life technologies, Cat# C34554). In brief, macrophages were incubated with 5 μM CFSE for 10 min and the rest CFSE was extensively removed. Subsequent, the cells were treated with 10 μM simvastatin equivalent [S]-rHDL or nothing for 24 hours. The percentage of proliferating cells of the total treated cells was determined by flow cytometry with a standard protocol.

Animals and diet

All animals were used based on an approved institutional protocol from Icahn School of Medicine at Mount Sinai. 5 weeks old male apoE-KO mice (B6.129P2-Apoe^{tm1Unc}) were

purchased from Jackson laboratory. All mice were fed with a high cholesterol diet, containing 20.3% fat, 22.9% protein, 45.7% carbohydrate and 0.2% cholesterol (Research Diets Inc., USA).

In vivo 9.4 Tesla MRI

To image the abdominal aortas, the mice were anesthetized and maintained by isoflurane containing air, and were subsequently scanned with a 9.4 Tesla MRI system (Bruker Instruments, Germany). T1-weighted MRI was performed using a black blood sequence. Twenty-two consecutive 500 μm thick slices with 500 μm inter-slice distance were acquired using a spin echo sequence with a 256X256 matrix size. A micro-scale in-plane resolution of 101 μm was achieved. The repetition time (TR) and echo time (TE) for the T1-weighted scanning were 800 and 8.6 ms, respectively. An inflow saturation band of 3 mm was used with a slice gap of 3 mm for additional luminal flow suppression. Sixteen signal averages were used for a total imaging time of 55 min per scan. A saturation pulse was used to eliminate signal from fat tissue and to delineate boundary of the aortic wall and minimize chemical shift artifacts. To investigate the plaque targeting of [S]-rHDL, mice were first subjected to baseline MRI scan, and subsequently injected through tail veins with a 50 μmol Gadolinium/kg dose of the [Gd-S]-rHDL. The mice were scanned again at 24 hours post-injection (N=3). Image analysis was done with semiautomatic software (VesselMass, Leiden) to delineate the aortic lumen area (LA) and outer wall area (OWA). Mean wall area (MWA) was defined as the difference between LA and OWA. The primary outcome parameter was the normalized wall index (NWI), which was calculated as: NWI = MWA / OWA. To evaluate the therapeutic effects of 12 week treatments, mice were scanned with the same protocol but without the injection of contrast agents.

Ex vivo near infrared fluorescence imaging (NIRF)

The mice were injected through tail veins with Cy5.5-DMPE and DiR labeled [S]-rHDL (N=3) or saline (N=3). At 24 hours post the injection, mice were sacrificed and perfused with PBS. To acquire Cy5.5 signal from [S]-rHDL in tissues, aortas, hearts, livers, spleens and kidneys were collected and imaged with IVIS 200 system (Xenogen) using 675(30) nm excitation and 720 (20) nm emission filters. Photon counts were used to quantify the fluorescence intensity from each tissue and it was reflected by color coded scale bar. Images were processed with the integrated software from IVIS 200 (Living Imaging Software 4.0). DiR signal was acquired with the same procedure but imaged at 745(30) nm excitation and 820 (20) nm emission filters.

Flow cytometry

To investigated the targeting mechanism of [S]-rHDL, apoE-KO mice were injected with Cy5.5 and DiO dual-labelled [S]-rHDL at dose of 15 mg/kg simvastatin and 10 mg/kg ApoA-1, the same as the low dose 12 week [S]-rHDL treatment. Mice were sacrificed at individual time points post injection (hour 1, 2, 4, 6, 12 and 24; N=3 per time point). Blood was collected and red blood cells were lysed and removed using red blood cell lysis buffer (BD Biosciences). Mice were perfused with PBS and cells from aortas were collected using the same method as described above. After perfusion with 30 ml of PBS, aortas were collected and the surrounding adipose tissue was removed carefully without damaging the

adventitia. Aortas were digested with 4 U/ml liberase LH (Roche), 0.1 mg/ml DNase I (Sigma-Aldrich), and 60 U/ml hyaluronidase (Sigma-Aldrich) in HBSS at 37°C for 90 min. The suspension was incubated with a mixture of monoclonal antibodies for 30 min at 4 °C. Fluorescence was detected by flow cytometer (BD Biosciences LSR II), and the data were analyzed using FlowJO software (Tree Star). Macrophages from aortas were identified as CD45+, CD11b+ and F4/80+, and monocytes were identified as CD45+, CD11b+, SSC-A low cells. Based on the Gr-1 expression, monocytes in the blood were further identified as Gr-1^{hi} and Gr-1^{lo} monocytes. To quantify the delivery efficiency to monocytes, macrophages and neutrophils in the spleen, a recently reported protocol was used[4]. Briefly, splenocytes were released by homogenizing the spleen and the tissue was digested with collagenase (Sigma-Aldrich) for 30 min at 37°C. A cocktail of antibodies include a Pacific blue-conjugated lineage (CD90 (clone 53-2.1), B220 (clone RA3-6B2), CD49b (clone DX5), NK1.1 (clone PK136), Ly-6G (clone 1A8) and Ter-119 (clone TER-119)), Alexa700 conjugated CD11b (clone M1/70), APC-conjugated CD11c (clone HL3), PE-Cy7 conjugated F4/80 (clone BM8) and PE-conjugated Ly6C (clone AL-21). Neutrophils were identified as Lineage high, CD11b high, ly-6c intermediate and SSC-A high. Macrophages were identified as lineage -, CD11b high, and F4/80 +. Monocytes were identified as Lineage -, CD11b high, CD11c −, F4/80 −, and Ly-6C +. Based on Ly-6c expression levels, monocytes were further identified as Ly-6c high and Ly-6c low monocytes. All antibodies were purchased from eBioscience, BD Biosciences and Biolegend and 1:200 dilution was used.

Fluorescence quantification of blood components

ApoE-KO mice received dual-labeled [S]-rHDL (Cy5.5 and DiO) through tail veins injection. At each individual time point (hour 1, 2, 4, 6, 12 and 24; N=3 per time point), mouse blood was drawn by cardiac puncture and stored in EDTA containing tubes. 500 μl blood was used for separating different compartments with Histopaque (Sigma-Aldrich, Histopaque 1077) by following the instructions from the manufacturer. Briefly, the blood and Histopaque solution was centrifuged at room temperature for 30 minutes, and three compartments from the blood (serum; mononuclear cells; red blood cells and granulocytes) were visible and collected. 50 μl solution from each compartment was added to 96-well plate (3 repeats for each condition). The plate was imaged with IVIS 200 system (Xenogen). To image DiO, excitation filter of 465 (30) nm and emission filter of 520 (20) nm were used. To image Cy5.5, excitation filter of 675 (30) nm and emission filter to 720 (20) nm were used. Signal intensity was analyzed and quantified using the integrated software from the system (Living Imaging Software 4.0).

Immunohistochemistry and image quantification

Serial 6 μm thick cross-sections were made of the aortic sinus area on a cryotome (Reichert HistoStat, Cryostat Microtome). From the first cross-section in which the leaflets of the aortic valves appeared upward, 63 serial cross-sections were obtained, covering the entire aortic sinus area. Of every 3 consecutive cross-sections, they were subjected to anti-CD68 immunohistochemical staining, hematoxylin phloxine saffron (HPS)-staining, and Oil Red O-staining. HPS (HPS, polyscientific) and Oil Red O-staining (Fisher Scientific) were done with standard methods. Anti-CD68-staining was done with a protocol previously reported[37].

The sections were blocked with rabbit serum (Vectorlabs), incubated for 1 hour with rat anti-mouse CD68 primary antibody (Abdserotec, 1:250 dilution), 10 minutes with biotinylated rabbit anti-rat antibody (Vectorlabs, 1:200 dilution), thereafter 5 minutes with VECTASTAIN ABC-alkaline phosphatase solution (Vectorlabs), and finally for 17 minutes with Vector Red solution (Vectorlabs).

All cross-sections were digitally imaged with a Nikon eclipse E400 microscope, with a 10x eyepiece and 10x lenses, a Nikon DS-U1 camera box and Nikon DS-5M camera. We used NIS-Elements F3.0 software, and imaged at a 1/350s exposure time, 2560 × 1920 pixels, and pixel size of 1.46 μm^2/ pix. Software written in Matlab was developed to facilitate automated image analysis.

Treatment protocol

For the 12 weeks of treatment study, 6 week old male apoE-KO mice were fed a high cholesterol diet (ResearchDiets, NJ) for 14 weeks, and subsequently received 12 weeks of intravenous injection of [S]-rHDL (15 mg/kg simvastatin, 10 mg/kg ApoA-1, 2 injections/ week, N=16), intravenous injection of rHDL (10 mg/kg ApoA-1, 2 injections/week, N=16), orally administered simvastatin (15 mg/kg/day, 2 saline intravenous injections/week, N=15) and placebo (2 saline injections/week, N=15). Mice were kept on a high fat diet during the 12 weeks treatment. Another group of mice (N=12) were sacrificed when the other groups started their 12 week treatment to establish a baseline. 8 mice per group were imaged with MRI over abdominal aortas before, in the middle and by the end of the 12 weeks treatments.

For one week short-term treatment study, 6 week old male apoE-KO mice were fed a high cholesterol diet for 27 weeks. After the diet, mice were injected intravenously with high dose [S]-rHDL (60 mg/kg simvastatin, 40 mg/kg ApoA-1, 4 injections /week), high dose rHDL (40 mg/kg ApoA-1, 4 injections /week), low dose [S]-rHDL (15 mg/kg simvastatin, 10 mg/kg ApoA-1, 4 injections /week) or placebo (4 saline injections/week).

Laser capture microdissection and qRT-PCR

36 male apoE KO mice with 6 weeks were fed a high fat diet for 26 weeks to develop advanced atherosclerosis. The animals received one week treatment of high dose [S]-rHDL (4 i.v. infusions of 60 mg/kg statin, 40 mg/kg ApoA1, denoted as “high [S]-rHDL), rHDL (2 i.v. infusions of 10 mg/kg ApoA1, denoted as “rHDL”), oral statin treatment (15 mg/kg/day oral simvastatin, denoted as “Oral SVS”), rHDL plus oral statin (15 mg/kg/day oral simvastatin and 2 i.v. infusions of 10 mg/kg ApoA1, denoted as “rHDL + Oral SVS”), or placebo (4 i.v. injections of PBS). Sections from aortic roots are prepared as described above, and a total of 24 sections were made per animal. For every 8 consecutive sections, the first one was stained with CD68 with the same method described above and used as the guiding section. The other 7 sections were used for isolating macrophages using laser capture microdissection (LCM) as previously described[35]. Briefly, the sections were fixed in 70% ethanol for 1 min, washed in H_2O, stained with Mayer’s hematoxylin (VWR Scientific) for 1 min, washed in H_2O, incubated in PBS (to develop blue color) for 15 seconds, washed in H_2O, partially dehydrated in 70% followed by 95% ethanol, stained in eosin Y (VWR Scientific) for 5 seconds, washed in 95% ethanol, and completely dehydrated in 100%

ethanol (30 seconds), xylene (30 sec) and xylene (5 minutes). After air-drying for 10 min, macrophages were identified under a microscope and be verified by the CD68 staining on the guiding slides. Several hundred macrophages per mouse were collected, and these macrophages from each animal were used to extract and amplify RNA with WT-Ovation Pico RNA amplification system (NuGen). The quality of extracted RNA was measured by Agilent 2100 Bioanalyzer. Quantitative Reverse Transcriptase PCR (qRT-PCR) was performed on samples using the iScript cDNA Synthesis kit (Bio Rad) according to manufacturer's protocol. The mRNA expression levels of investigated genes were normalized to housekeeping gene hprt1 (UniGene ID: Mm.1037830). The following genes were investigated: MCP-1 (Mm.290320), CCL-3 (Mm.1283), ICAM-1 (Mm.435508), VACM-1 (Mm.440909), CXCL12 (Mm.303231), CCL15 (Mm.284348), TNF-α (Mm. 1293), IL-1β (Mm.222830), IL-1α (Mm.15534), Spp1 (Mm.288474), MR (Mannose Receptor, Mm2019). TaqMan Gene Expression assay (Life Technologies, Cat. NO. 4331182) was used to measured the gene expression on sequence detection device (ABI PRISM 7900HT).

Fluorescence molecular tomography with CT

Eleven 6 week old apoE-KO mice were fed a high fat diet for 20 weeks before receiving 4 high dose [S]-rHDL or placebo (PBS) injections in a week. Five nmol of pan-cathepsin protease sensor (ProSense 680, PerkinElmer, Cat# NEV10003) was intravenously administered along with the last intravenous injection of [S]-rHDL or PBS. 24 hours later the animals were placed in a custom-built imaging cartridge which was equipped for isoflurane administration during imaging. Animals were first scanned with high-resolution computated tomography (CT; Inveon PET-CT, Siemens), with a continuous infusion of CT-contrast agent (isovue-370, Bracco Diagnostics) at a rate of 55 μl/min through a tail-vein catheter. Animals were subsequently scanned with an FMT scanner (PerkinElmer) in the same cartridge. The CT x-ray source with an exposure time of 370–400 ms was operated at 80kVp and 500 μA. Contrast-enhanced high resolution CT images were used to localize the aortic root, which was used to guide the placement of the volume of interest for the quantitative FMT protease activity map. The CT reconstruction protocol involved bilinear interpolation, used a Shepp-Logan filter, and scaled pixels to Hounsfiled units. Image fusion relied on fiducial markers and used Osirix software (The Osirix Foundation, Geneva).

Blood tests and lipoprotein analysis

After 4 hours of fasting, whole blood was collected in EDTA containing tube. Some serum was subjected to a biochemistry panel (ALX laboratories, NY) analysis to determine the blood concentrations of alanine transaminase, aspartate transaminase, creatinine, creatine kinase, cholesterol and triglyceride. The rest serum was pooled per group for lipoprotein analysis via fast performance liquid chromatography (FPLC) (Pharmacia). For each sample, 250 μl of plasma was applied to 2 Superose 6 columns (GE healthcare) equilibrated and run in a buffer containing 150 mM NaCl and 15 mM EDTA in deionized water. The column flow rate was 0.7 mL/min. 80 fractions were collected, and the total cholesterol concentration of each fraction was assessed by enzymatic colorimetric assay (Wako) according to the manufacturer's instructions.

Cholesterol measurement in thoracic aorta

The thoracic aortas were blotted dry and weighed. Later, they were minced and extracted with chloroform/methanol (2:1) according to the method of Folch *et al*.[36] The cholesterol containing supernatant was measured (WACO diagnostics) and the total cholesterol from the aortas was calculated accordingly. Finally, the ratio of cholesterol to tissue was calculated by dividing the total cholesterol content per aorta by the weight of the aorta.

Statistics

Continuous variables are expressed as means ± standard deviation, unless otherwise stated. Significance of differences was calculated by use of the nonparametric Mann-Whitney U tests and Kruskal-Wallis tests. Multiple linear regression analysis was used to assess the association between CD68 area and the various treatment groups, with CD68 area as the response variable and treatment group as the explanatory variable, adjusting for the potential confounder serum total cholesterol. Composite variables were calculated for monocyte recruitement and pro-inflammatory mRNA expression in the LCM experiment. Probability values of $P<0.05$ were considered significant. Statistical analyses were done using SPSS (Statistical Package for the Social Sciences) version 17.0 and SAS package (SAS Institute Inc.).

Supplementary Material

Refer to Web version on PubMed Central for supplementary material.

Acknowledgments

The authors would like to thank S. Russell for helping with the FPLC experiments and Wei Chen for his contribution to the flow cytometry experiments. R. Nolasco is gratefully acknowledged for his help in cryosectioning the aorta specimens and CSL (Parkville, Australia) for their kind gift of ApoAI.

This work was supported by the NHLBI, NIH, as a Program of Excellence in Nanotechnology (PEN) Award, Contract #HHSN268201000045C as well as the NIH grants R01 EB009638 (Z.A.F.), K99 EB012165 (D.P.C.), R01 CA155432 (W.J.M.M.), P01HL098055 (E.A.F.), R01HL084312 (E.A.F.) and the NWO grant ZonMW Vidi 91713324 (W.J.M.M.). Additional support was provided by the American Heart Association Award #13PRE14350020-Founders (J.T.), the Deutsche Forschungsgemeinschaft #SA 1668/2-1 (H.S.), the German Research Foundation DFG #HE 6092/1-1 (B.H.)as well as by the International Atherosclerosis Society and by the Foundation “De Drie Lichten” in The Netherlands (M.E.L). Flow cytometry was performed at the MSSM-Flow Cytometry Shared Resource Facility and RT-PCR at Quantitative PCR Shared Resource Facility. Fluorescence microscopy was performed at the MSSM-Microscopy Shared Resource Facility, supported with funding from NIH-NCI shared resources grant (5R24 CA095823-04), NSF Major Research Instrumentation grant (DBI-9724504) and NIH shared instrumentation grant (1 S10 RR0 9145-01).

References

1. Grundy SM, et al. National Heart, Lung, and Blood Institute; American College of Cardiology Foundation; American Heart Association. Implications of recent clinical trials for the National Cholesterol Education Program Adult Treatment Panel III guidelines. Circulation. 2004; 110:227–39. [PubMed: 15249516]
2. Libby P. The forgotten majority: unfinished business in cardiovascular risk reduction. J Am Coll Cardiol. 2005; 46:1225–8. [PubMed: 16198835]
3. Milonas C, et al. Effect of angiotensin-converting enzyme inhibition on one-year mortality and frequency of repeat acute myocardial infarction in patients with acute myocardial infarction. Am J Cardiol. 2010; 105:1229–1234. [PubMed: 20403471]

4. Dutta P, et al. Myocardial infarction accelerates atherosclerosis. Nature. 2012; 487:325–329. [PubMed: 22763456]
5. Libby P, Ridker PM, Hansson GK. Progress and challenges in translating the biology of atherosclerosis. Nature. 2011; 473:317–325. [PubMed: 21593864]
6. van der Wal AC, Becker AE, van der Loos CM, Das PK. Site of intimal rupture or erosion of thrombosed coronary atherosclerotic plaques is characterized by an inflammatory process irrespective of the dominant plaque morphology. Circulation. 1994; 89:36–44. [PubMed: 8281670]
7. Weber C, Noels H. Atherosclerosis: current pathogenesis and therapeutic options. Nature Med. 2011; 17:1410–1422. [PubMed: 22064431]
8. Goldstein JL, Brown MS. Regulation of the mevalonate pathway. Nature. 1990; 343:425–30. [PubMed: 1967820]
9. Kwak B, Mulhaupt F, Myit S, Mach F. Statins as a newly recognized type of immunomodulator. Nature Med. 2000; 6:1399–402. [PubMed: 11100127]
10. Weitz-Schmidt G, et al. Statins selectively inhibit leukocyte function antigen-1 by binding to a novel regulatory integrin site. Nature Med. 2001; 7:687–92. [PubMed: 11385505]
11. Pahan K, Sheikh FG, Namboodiri AM, Singh I. Lovastatin and phenylacetate inhibit the induction of nitric oxide synthase and cytokines in rat primary astrocytes, microglia, and macrophages. J Clin Invest. 1997; 100:2671–9. [PubMed: 9389730]
12. Sparrow CP, et al. Simvastatin Has Anti-Inflammatory and Antiatherosclerotic Activities Independent of Plasma Cholesterol Lowering. Arterioscler Thromb Vasc Biol. 2001; 21:115–121. [PubMed: 11145942]
13. Armitage J. The safety of statins in clinical practice. Lancet. 2007; 370:1781–90. [PubMed: 17559928]
14. Bellosta S, Paoletti R, Corsini A. Safety of statins: focus on clinical pharmacokinetics and drug interactions. Circulation. 2004; 109:III50–7. [PubMed: 15198967]
15. Bell FP. Lipid exchange and transfer between biological lipid-protein structures. Proq Lipid Res. 1978; 17:207–43.
16. Skajaa T, et al. Quantum Dot and Cy5.5 Labeled Nanoparticles to Investigate Lipoprotein Biointeractions via Förster Resonance Energy Transfer. Nano Lett. 2010; 10:5131–38. [PubMed: 21087054]
17. Skajaa T, et al. The biological properties of iron oxide core high-density lipoprotein in experimental atherosclerosis. Biomaterials. 2011; 32:206–13. [PubMed: 20926130]
18. Osada J, Joven J, Maeda N. The value of apolipoprotein E knockout mice for studying the effects of dietary fat and cholesterol on atherogenesis. Curr Opin Lipidol. 2000; 11:25–9. [PubMed: 10750690]
19. Quarfordt SH, et al. *In vivo* cholesterol kinetics in apolipoprotein E-deficient and control mice. J Lipid Res. 1995; 36:1227–35. [PubMed: 7666000]
20. Vyas KP, Kari PH, Prakash SR, Duggan DE. Biotransformation of lovastatin. II. *In vitro* metabolism by rat and mouse liver microsomes and involvement of cytochrome P-450 in dehydrogenation of lovastatin. Drug Metab Dispos. 18:218–22. [PubMed: 1971576]
21. Rader D. Molecular regulation of HDL metabolism and function: implications for novel therapies. J Clin Invest. 2006; 116:3090–3100. [PubMed: 17143322]
22. Tall AR, Yvan-Charvet L, Terasaka N, Pagler T, Wang N. HDL, ABC transporters, and cholesterol efflux: implications for the treatment of atherosclerosis. Cell Metab. 2008; 7:365–75. [PubMed: 18460328]
23. Shah PK, et al. Effects of recombinant apolipoprotein A-I(Milano) on aortic atherosclerosis in apolipoprotein E-deficient mice. Circulation. 1998; 97:780–5. [PubMed: 9498542]
24. Shah PK, et al. High-dose recombinant apolipoprotein A-I(milano) mobilizes tissue cholesterol and rapidly reduces plaque lipid and macrophage content in apolipoprotein e-deficient mice. Potential implications for acute plaque stabilization. Circulation. 2001; 103:3047–50. [PubMed: 11425766]
25. Nissen SE, et al. Effect of recombinant ApoA-I Milano on coronary atherosclerosis in patients with acute coronary syndromes: a randomized controlled trial. JAMA. 2003; 290:2292–300. [PubMed: 14600188]

26. Tardif JC, et al. Effects of reconstituted high-density lipoprotein infusions on coronary atherosclerosis: a randomized controlled trial. JAMA. 2007; 297:1675–82. [PubMed: 17387133]
27. Vaisar T, et al. Shotgun proteomics implicates protease inhibition and complement activation in the antiinflammatory properties of HDL. J Clin Invest. 2007; 117:746–56. [PubMed: 17332893]
28. Vickers KC, Palmisano BT, Shoucri BM, Shamburek RD, Remaley AT. MicroRNAs are transported in plasma and delivered to recipient cells by high-density lipoproteins. Nat Cell Biol. 2011; 13:423–33. [PubMed: 21423178]
29. Liao JK. Isoprenoids as mediators of the biological effects of statins. J Clin Invest. 2002; 110:285–8. [PubMed: 12163444]
30. Jain MK, Ridker PM. Anti-inflammatory effects of statins: clinical evidence and basic mechanisms. Nat Rev Drug Discov. 2005; 4:977–87. [PubMed: 16341063]
31. Lobatto ME, Fuster V, Fayad Za, Mulder WJM. Perspectives and opportunities for nanomedicine in the management of atherosclerosis. Nat Rev Drug Discov. 2011; 10:835–52. [PubMed: 22015921]
32. Jonas ANA. Apolipoproteins. Methods. 1986; 128:553–582.
33. Forte T. Electron microscopy of negatively stained lipoproteins. Methods Enzymol. 1986; 128:442–457. [PubMed: 2425222]
34. Carlucci G, Mazzeo P, Biordi L, Bologna M. Simultaneous determination of simvastatin and its hydroxy acid form in human plasma by high-performance liquid chromatography with UV detection. J Pharm Biomed Anal. 1992; 10:693–7. [PubMed: 1286134]
35. Trogan E, et al. Laser capture microdissection analysis of gene expression in macrophages from atherosclerotic lesions of apolipoprotein E-deficient mice. Proc Natl Acad Sci USA. 2002; 99:2234–9. [PubMed: 11842210]
36. Folch J, Lees M, Sloane Stanley GH. A simple method for the isolation and purification of total lipides from animal tissues. J Biol Chem. 1957; 226:497–509. [PubMed: 13428781]

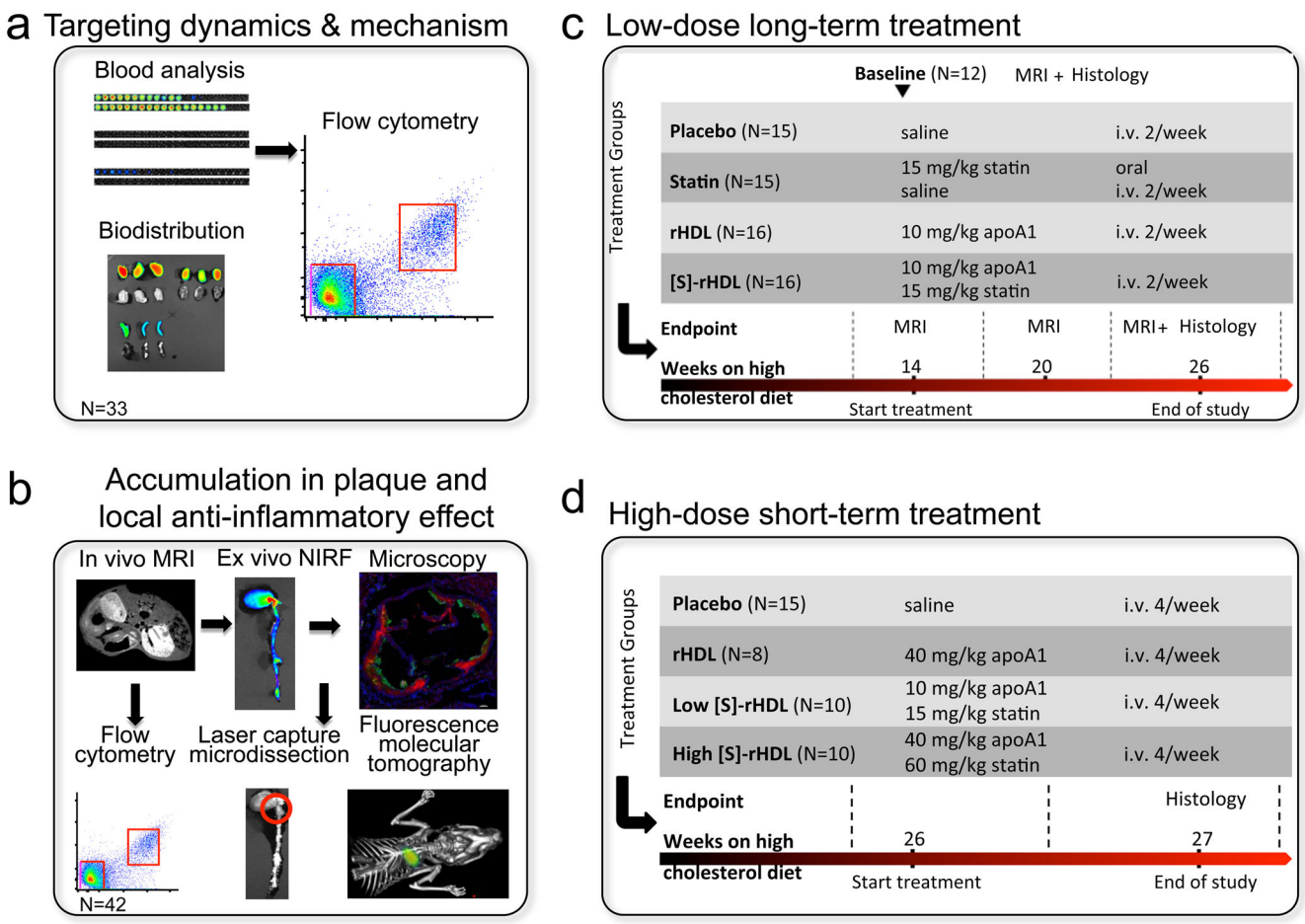

Figure 1. Schematic of the study design

(a) The targeting dynamics, targeting mechanism and anti-inflammatory action of [S]-rHDL in apoE-KO mice were investigated by analyzing the dynamics of phospholipids and hydrophobic cargos of [S]-rHDL in the blood by NIRF and flow cytometry. The biodistribution was evaluated in organs with NIRF. (b) Magnetic resonance imaging (MRI), near infrared fluorescence imaging (NIRF), fluorescence microscopy, and flow cytometry were used to validate the plaque macrophage targeting efficiency of [S]-rHDL. The effect of [S]-rHDL on the mRNA levels of inflammatory genes of plaque macrophages were determined in macrophages isolated with laser capture microdissection. Fluorescence molecular tomography and computed tomography was used to assess the effect of [S]-rHDL on inflammatory protease activity in aortic root plaques. (c) The efficacy of low-dose long-term (12 weeks) [S]-rHDL treatment on disease progression was evaluated in the abdominal aortas with MRI and in aortic roots with histology. (d) The efficacy of high-dose short-term (1 week) [S]-rHDL treatment was evaluated in aortic roots with histology.

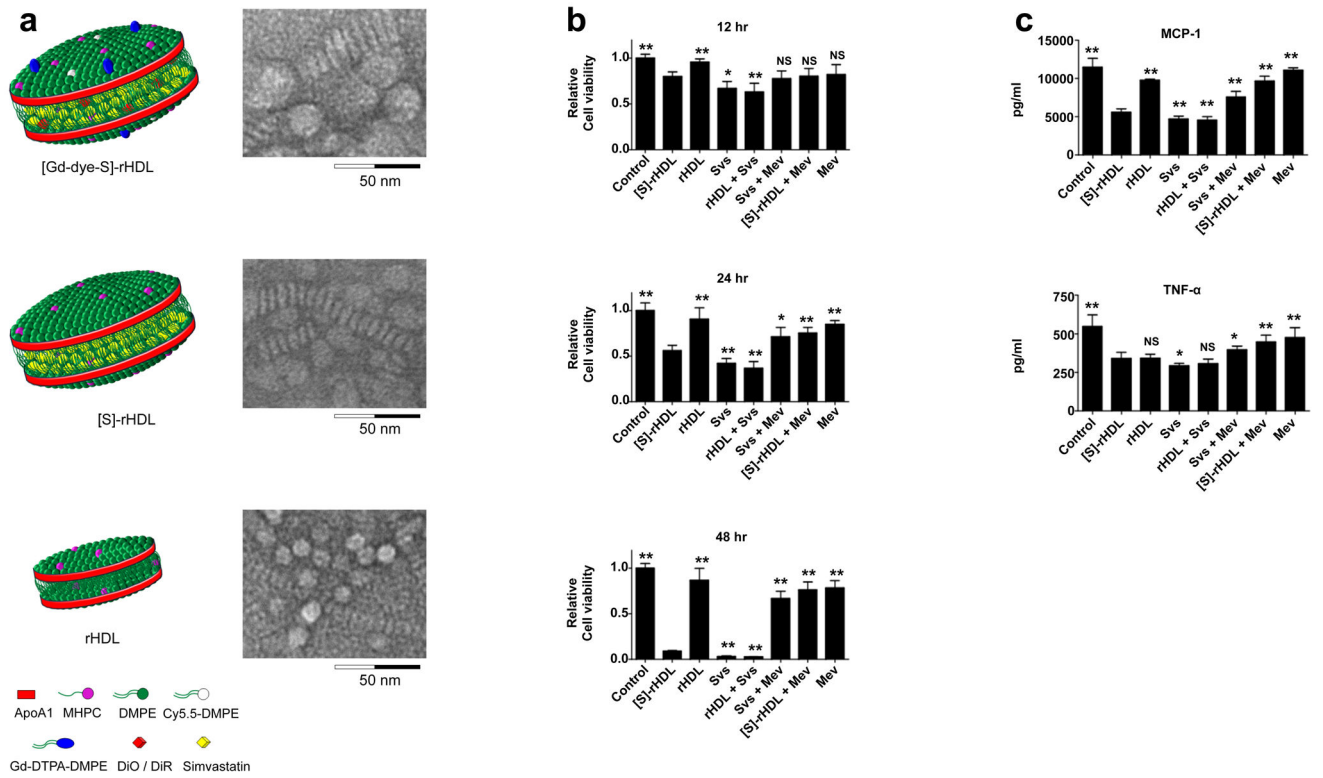

Figure 2. Schematic representations of the nanoparticle formulations and *in vitro* efficacy data

(a) Schematic representation of dual gadolinium and fluorescent dye (Cy5.5, DiO, DiR) labeled statin containing reconstituted high density lipoprotein ([Gd-dye-S]-rHDL), statin containing rHDL ([S]-rHDL), and rHDL. Negative staining transmission electron microscopy (TEM) images of each of the aforementioned particles showed the typical disk-like morphology. The circular shapes are nanoparticles viewed en face, while the striped configurations are rouleaux of nanoparticles viewed from the side. Dynamic light scattering measurements showed the average size of [Gd-dye-S]-rHDL to be 28.5 nm, of [S]-rHDL to be 26.0 nm and of rHDL to be 10.5 nm. For larger view TEM also see Supplementary Fig. S1. (b) *In vitro* cell viability assays of murine macrophages (J774A.1), incubated with combinations of [S]-rHDL (10 μM statin) free simvastatin (10 μM), rHDL plus free statin (10 μM), free statin (10 μM) plus mevalonate (100 μM), [S]-rHDL (10 μM) plus mevalonate (100 μM), and only mevalonate (100 μM). There was also a control group of cells not incubated with anything. Macrophage cell viability is markedly decreased in the [S]-rHDL and free statin group. This effect is abolished by addition of mevalonate, indicating that the effect of HMGR inhibition on cell viability is mediated through the mevalonate pathway. N=6 for all bars. (c) Production of the inflammatory cytokines MCP-1 and TNF-α. LPS and INF-γ challenged macrophages were incubated with the same treatments as mentioned above for 24 hours. MCP-1 and TNF-α levels are markedly reduced by [S]-rHDL and free statin. MCP-1 and TNF-α levels are restored by the addition of mevalonate to [S]-rHDL and free statin incubation. N=6 for all bars. Cell viability in the different groups was not affected under these conditions (Supplementary Fig. S4). All error bars are 95% confidence intervals. P-values are calculated with Mann-Whitney U tests for comparisons with [S]-rHDL, * indicates $P < 0.05$, ** indicates $P < 0.01$. Kruskal-Wallis P-values are < 0.0001 for all plots.

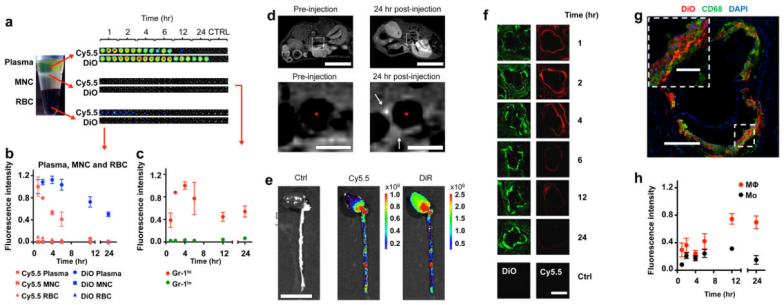

Figure 3. Pharmacokinetics and accumulation in plaque of labeled nanoparticles

(a) Cy5.5- and DiO-labelled [S]-rHDL was intravenously injected to apoE-KO mice (N=21, 3 mice per time point) and blood and tissues were analyzed at different time points post-injection. NIRF shows that components from the lipid monolayer (Cy5.5) have much shorter blood half-life than components from hydrophobic core (DiO). It also shows that the majority of [S]-rHDL stays in serum and very little in red blood cells (RBC) and mononuclear cells (MNC). (b) Fluorescence intensity in serum, MNC, and RBC is quantified (N=21, 3 mice per time point). We calculated that plasma half-life of [S]-rHDL to be 21.9 hours for the DiO signal. (c) Flow cytometric analysis of blood cells shows that [S]-rHDL targets Gr-1^{hi} pro-inflammatory monocytes more efficiently than Gr-1^{lo} anti-inflammatory monocytes in blood (N=21, 3 mice per time point). (d) Typical T1-weighted 9.4 Tesla magnetic resonance images of the abdominal aorta of an apoE-KO mouse, made at identical locations, before and 24 hours after injection of [Gd-Dye-S]-rHDL. The lumen is indicated by *. The scale bar in the upper images represent 10 mm, and in the lower images 1 mm. The 24h post-injection image showed signal enhancement in the vessel wall (white arrows), indicative of nanoparticle infiltration and retention in the aortic plaques. (e) [S]-rHDL labeled with Cy5.5 (lipid monolayer) and DiR (hydrophobic core) was intravenously injected to apoE-KO mice. NIRF shows that Cy5.5 and DiR preferentially accumulates in the areas rich with atherosclerotic lesions. The scale bar represent 10 mm. (f) Cy5.5 and DiO both appear in the plaque, until 4 hours post-injection the presence of Cy5.5 declines while DiO remains present. The scale bar represents 500 μm. (g) DiO-labelled [S]-rHDL co-localizes in the plaque with CD68 (macrophages). The scale bar in the inset represent 100μm, and in the overview 400 μm (h) Flow cytometric analysis of cells in aorta walls shows that [S]-rHDL is taken up by plaque macrophages, furthermore, macrophages are targeted more efficiently than monocytes (N=3 per timepoint). All error bars are standard errors of the mean.

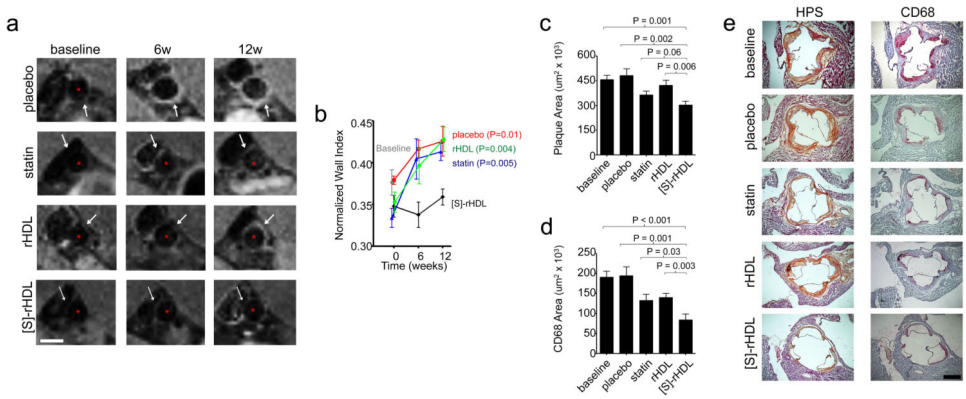

Figure 4. *In vivo* efficacy of 12 weeks biweekly low dose [S]-rHDL infusions

(a) Efficacy of [S]-rHDL on abdominal atherosclerosis quantified by 9.4 Tesla magnetic resonance imaging (9.4T-MRI). Typical T1-weighted MR images of the abdominal aortas of mice in each group at all time points show the thickening of the aorta wall in all groups except in the [S]-rHDL-treated group. The analysis method of the images is shown in Supplementary Fig. S9. The scale bar represents 1 mm. (b) MRI scans of the abdominal aortas of 32 mice (N=8 per group) were performed at three time points during the study. When the apoE-KO mice were 14 weeks on high cholesterol diet the baseline scans were acquired and subsequent scans were performed 6 and 12 weeks after the baseline scan. From baseline onwards the mice received placebo, oral statin therapy, or injections of reconstituted high-density lipoprotein (rHDL) or statin containing rHDL ([S]-rHDL). Thickness of the vessel wall is expressed as the normalized wall index (NWI), which is defined as the ratio between the mean wall area and the outer wall area. (c) Efficacy of [S]-rHDL assessed by histology shows that mean plaque area was lower in the [S]-rHDL treated group (N=15) as compared to placebo (N=16) and rHDL (N=16), and there was a trend towards decreased plaque area compared to statin therapy (N=15). Kruskal-Wallis P-value for plaque area is 0.0011. (d) Plaque macrophage content as measured by the CD68 positive area was decreased in the [S]-rHDL group (N=15) as compared to placebo- (N=16), statin- (N=15) and rHDL-therapy (N=16), indicating decreased plaque inflammation in the [S]-rHDL group. Bars represent the standard error of the mean, P-values were calculated with Mann-Whitney U tests. Kruskal-Wallis P-value for CD68 area is 0.0001. (e) Typical histology images of the aortic sinus area of each group are shown. The hematoxylin phloxine saffron (HPS)-stained images are shown on the left and the cross-sections stained with CD68 antibodies are shown on the right. The analysis method of the histology images is shown in Supplementary Fig. S9. The scale bar represents 400 μm.

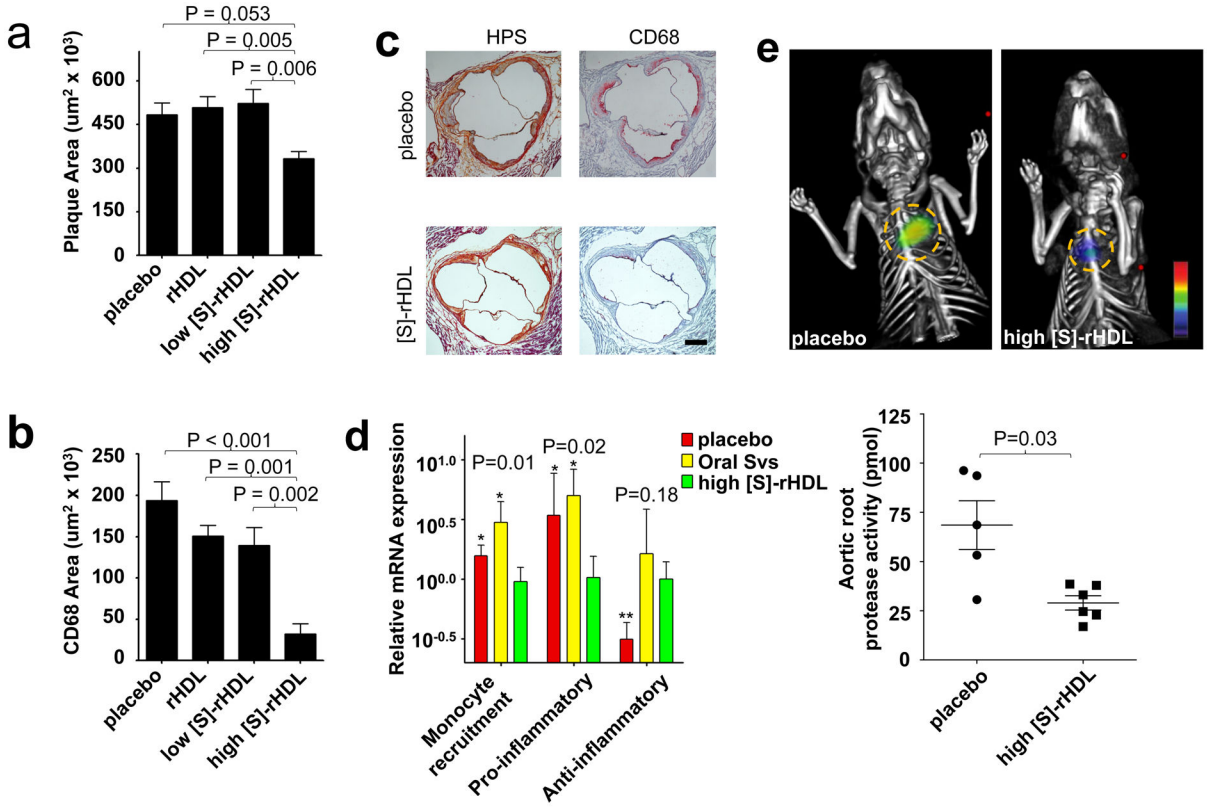

Figure 5. ***In vivo*** **efficacy of a single week high dose [S]-rHDL infusions**

(a) Mean plaque area was lower in the high dose [S]-rHDL-treated group (N=10) as compared to placebo (N=15), high dose rHDL (N=8), and low dose [S]-rHDL(N=10). Kruskal-Wallis P-value for plaque area is 0.037. (b) Plaque macrophage content as measured by the CD68 positive area was decreased in the high dose [S]-rHDL (N=10) as compared to placebo (N=15), high dose rHDL (N=8), and low dose [S]-rHDL (N=10), indicative of decreased plaque inflammation in this group. Bars represent the standard error of the mean, P-values were calculated with Mann-Whitney U tests. Kruskal-Wallis P-value for CD68 area is 0.0006. (c) Typical histology images of the aortic sinus area from a mouse in the placebo group and a mouse in the high dose [S]-rHDL-group show that mean plaque area is similar, while the plaque macrophage content is notably smaller in the [S]-rHDL-group. The hematoxylin phloxine saffron (HPS)-stained images are shown on the left and the cross-sections stained with CD68 antibodies are shown on the right. The scale bar represents 400 μm. (d) One-week high dose [S]-rHDL treatment (N=6) significantly reduced the mRNA expression levels of monocyte recruitment genes (composite variable of MCP-1, CCL-3, ICAM-1, VCAM-1, CCL-15, CXCL-12) and pro-inflammatory genes (composite variable of TNF-α, IL-1β, IL-1α, SPP-1) of plaque macrophages in the aortic root when compared to placebo (N=6) and oral statin (N=6). The expression of the anti-inflammatory mRNA level (MR) was increased in the high dose [S]-rHDL group as compared to placebo, but not compared to oral statin therapy. P-values are calculated with Mann-Whitney U tests for comparisons with [S]-rHDL, * indicates $P < 0.05$, ** indicates $P < 0.01$. Kruskal-Wallis P-values are shown in the plot. The error bars represent the standard deviations. (e) FMT-CT molecular imaging of protease activity revealed that high dose [S]-rHDL treatment (N=6) significantly reduced the inflammation levels in the aortic roots of live apoE-KO mice with advanced atherosclerosis as compared to placebo (N=5). The yellow circles indicate the aortic root area. The error bars represent the standard error of the mean. P-values were calculated with the Mann-Whitney U test.